Ag-TON nanospheres coupled with fly ash cenospheres for wastewater treatment under visible light irradiation

Yan Ma, Zhihuan Zhao, Jimin Fan, Zhanyong Gu, Bin Zhang and Shu Yin

ABSTRACT

Using tetra-n-butyl titanate as raw material and fly ash cenospheres (FAC) as carrier, the photocatalysts of Ag-TON/FAC were successfully prepared by solvothermal and in-situ hydrolysis method. These visible light photocatalysts were characterized by X-ray diffraction (XRD), scanning electron microscopy (SEM), fluorescence spectroscopy (FL) and UV–vis diffuse reflectance spectra (DRS). In this study, methyl orange and ciprofloxacin were used as wastewater degradation targets to investigate the effect of the amount of titanium dioxide and the amount of Ag doping on the activity of photocatalysts. On the basis of this, the optimal ratio of TiO_2 to FAC was 2:1 and the optimum doping ratio of Ag was determined to be 15 wt.%. The composite photocatalysts dispersed uniformly and were easy to recycle and reuse, which were benefits in fully utilizing the solar energy. The degradation efficiency remained at more than 60% after being renewed five times for MO and ciprofloxacin. The photocatalysts of Ag-TON/FAC can reduce the environmental burden caused by FAC also.

Key words | fly ash cenospheres, photocatalytic activity, visible light, wastewater treatment

Yan Ma
Zhihuan Zhao (corresponding author)
Jimin Fan
Bin Zhang
College of Chemistry and Chemical Engineering,
Taiyuan University of Technology,
Taiyuan, Shanxi,
China
E-mail: *zzh1972129@163.com*

Zhanyong Gu
Shu Yin
Institute of Multidisciplinary Research for Advanced Materials,
Tohoku University,
2-1-1, Katahira, Aoba-ku, Sendai 980-8577,
Japan

INTRODUCTION

Nowadays, wastewater is the most concerning problem worldwide that humankind faces due to population growth and the development of industrialization. From the environmental point of view, wastewater is threatening human health and the environment on which it depends. Wastewater treatment and reuse, hence, have become the main target to protect the environment around the world (Ibrahim & Asal 2017). Photocatalytic oxidation is an advanced oxidation technology developed in the past 30 years, which has attracted considerable attention. For example, Kanakaraju & Wong (2018) prepared a novel TiO_2/modified sago bark mixture for wastewater treatment and the experimental results proved its feasibility for wastewater treatment. Fang *et al.* (2018) synthesized Fe(VI)-Fe_3O_4/graphene nanocomposites by a co-precipitation method in order to degrade ciprofloxacin. The results demonstrated that the Fe(VI)-Fe_3O_4/graphene system could offer an alternative process in wastewater treatment. Yu *et al.* (2018) also prepared Z-scheme AgI/BiOBr composites, and they exhibited a rapid photocatalytic oxidation ability for ciprofloxacin with a removal efficiency of 90.9% under visible light. However, there are some unfavorable factors in the nanoparticles application process, such as the high recombination of photoexcited electrons and holes (Marques *et al.* 2017), the narrow light absorption regions of ultraviolet and near ultraviolet (Achamo & Yadav 2016), the poor adsorption capacity for target pollutants (Zhou *et al.* 2016), inefficient use of visible light, being hard to recycle (Chen *et al.* 2017; Wang *et al.* 2018a, 2018b) and so on. Especially, separation and recovery of nanopowder TiO_2 is difficult (Wu *et al.* 2010). Hence, there are many approaches that have been proposed to improve the performance of semiconductor catalysts, such as being compounded with other semiconductors (Wang *et al.* 2018a, 2018b), increasing the particle size (Sieland *et al.* 2018) and being composed with carriers (Zhang *et al.* 2017), etc. For example, Wang *et al.* (2011) deposited Fe^{3+} doped TiO_2 film on fly ash cenospheres (Fe–TiO_2/FAC) by a sol-gel method and these were used to degrade methyl blue (MB) under visible light. Ma *et al.* (2017) successfully prepared porous polyvinyl alcohol-TiO_2 spheres by a phase inversion method. The surface area of the spheres was 200 m^2/g, and porous spheres could be used for methyl orange water treatment. Tang *et al.* (2018) synthesized large surface area nanofibers of TiO_2/g-C_3N_4 by a one-step electrospinning method and the nanofibers showed a high degradation rate to rhodamine B.

doi: 10.2166/wst.2018.513

These studies offer a promising future to solve the problems of wastewater.

Fly ash cenospheres, aluminosilicate-rich by-products, are generated in coal-firing powder plants that bring great challenges to the environment (Huo *et al.* 2011). A potential environmental application of these by-products will make them a resource rather than a castoff (Papoulis *et al.* 2014). As we reported earlier, the main chemical components of FAC were SiO_2, Al_2O_3, Fe_2O_3, TiO_2 and MgO, etc. (Zhao *et al.* 2017). Generally, glass cenospheres account for a large proportion, magnetite accounts for 6–16%, and carbon particles account for 4–18%. FAC have strong adsorption properties with large specific surface and it is easily dispersed and recycled from wastewater for its hollow structure. When TiO_2 is supported on FAC, its dispersibility increases and TiO_2 can be recycled efficiently; at the same time its agglomeration will be prevented. FAC are the ideal carrier for TiO_2 because of their unique structure. In addition, the use of FAC can also solve environmental problems.

In this study, Ag and N codoped TiO_2 is coated onto the surface of FAC by a solvothermal and in-situ hydrolysis method. Consequently, the photocatalysts of Ag-TON/FAC can be easily separated from wastewater. Furthermore, the photocatalytic performance of the as-synthesized samples is investigated by testing the degradation activity of methyl orange (MO) and ciprofloxacin wastewater.

EXPERIMENT

Materials and chemicals

Tetrabutyl titanate (TBOT, $C_{16}H_{36}O_4Ti$, AR), ethanol (C_2H_5OH, AR), polyethylene glycol (PEG, AR) and methyl orange (MO, AR) were used without further purification. FAC were collected from Taiyuan thermal power plant and were sieved with 200 mesh (particle size $\leq$74 μm), and then treated with 86 ml of 10% dilute nitric acid for 12 h to clean the surface. Next, the suspension was filtered and washed with deionized water several times until pH = 7, and then the product was dried in a vacuum at 60 °C overnight. The other chemical reagents were analytical grade.

Preparation of Ag-TON/FAC

The photocatalysts of Ag-TON/FAC were prepared by a solvothermal and in-situ hydrolysis method. In a typical process, the titanium tetra-n-butoxide was dissolved in ethanol as the raw material and stirred for 30 min, then named solution A. Solution B was the mixture solution of deionized water, nitric acid, silver nitrate (Ag:TiO_2 = 1 wt.%, 8 wt.%, 10 wt.%, 15 wt.%, 20 wt.%) and 1.2 g urea. Then solution B was added dropwise into solution A and continuously stirred for 30 min to obtain the mixture solution. 2 g polyethylene glycol was dropped into the mixture solution at 50 °C with stirring for 30 min. The pre-treated FAC were added, also at room temperature, and stirred for another 30 min. Next, the solution was transferred into a 100 ml Teflon-lined stainless steel autoclave, heated at 90 °C for 1 h, and then heated to 190 °C for 2 h. Subsequently, the products were centrifuged and washed with deionized water and ethanol six times respectively, and dried in a vacuum at 60 °C overnight. Finally, the powder was calcined at 450 °C for 2 h. The quality ratio of TiO_2 to FAC was 2:1, 1:1, 1:2 and 1:3. The obtained samples were denoted as Ag-TON/FAC.

For comparison, under the same experimental conditions, N-TiO_2/FAC was prepared without adding silver nitrate; TiO_2/FAC was obtained without adding urea; TiO_2 was prepared without adding FAC.

Sample characterization

The crystallographic analysis of the sample was performed using a D/MAX-2500 X-ray diffractometer (XRD) manufactured by RIGAKU of Japan. UV–vis spectrophotometer (LambdaBio40, PE, USA) was used to measure UV–vis diffuse reflectance spectra (DRS) of the samples. The fluorescence spectra (FL) was measured by Hitachi F-2700 fluorescence spectrophotometer (Japan). The size and morphology of the particles were observed by scanning electron microscope (SEM; Hitachi S-4800).

Photocatalytic activity test

The experiment was carried out at room temperature. A 300 W Xe lamp equipped with a 400 nm cut-off filter was used as a light source. In the experiment, 0.2 g and 0.02 g of the as-prepared sample were dispersed in 50.0 mL of MO and ciprofloxacin solution (20 mg L^{-1}), respectively. The distance between the reactor containing the reaction mixture and the light source was 12 cm. Before the irradiation, the target aqueous solution was stirred for half an hour in the dark to achieve the adsorption-desorption balance. Sampling analysis was conducted every 15 min and centrifuged to remove the sample

particles. The MO/ciprofloxacin concentration was monitored by recording the maximum absorbance at 466 nm/272 nm with a UV–vis spectrophotometer.

RESULTS AND DISCUSSION

Figure 1(a) shows the XRD patterns of TiO_2, TiO_2/FAC, N-TiO_2/FAC and Ag-TON/FAC. As shown in Figure 1, all the as-synthesized samples showed anatase phase TiO_2 with characteristic diffraction peaks. The 2θ diffraction peaks at 25.3°, 37.0°, 37.8°, 38.6°, 48.1°, 54.1°, 54.9°, 62.7°, 68.9°, 70.3° and 75.1° correspond to the planes of (101), (103), (004), (112), (200), (105), (211), (204),(116), (220) and (215), respectively. It is obvious that pure TiO_2 has a partially crystalline rutile crystal structure. The peaks at 27.5° and 36.1° correspond to rutile phase (110) and (101) lattice plane (JCPDS 78-1508). The sample of Ag-TON/FAC has both characteristic peaks of FAC and TiO_2. The diffraction peaks appear at 38.1°, 44.3° and 64.2°, assigned to the metallic Ag in the face-centered cubic structure (JCPDS 87-0718), indicating that the sample container metallic silver (Padmanaban *et al.* 2017). The XRD pattern shows that doping of Ag and N will not change the crystal phase of TiO_2. The average particle size of the samples is within the nano range. The nanometer size will increase the surface area of the photocatalyst, resulting in an ideal photocatalytic activity.

UV–vis reflectance spectra and Kubelka–Munk plots (the inset) of all as-synthesized samples are shown in Figure 1(b). It can be seen from Figure 1(b) that the band gap of TiO_2 is 3.20 eV, which can only absorb the ultraviolet

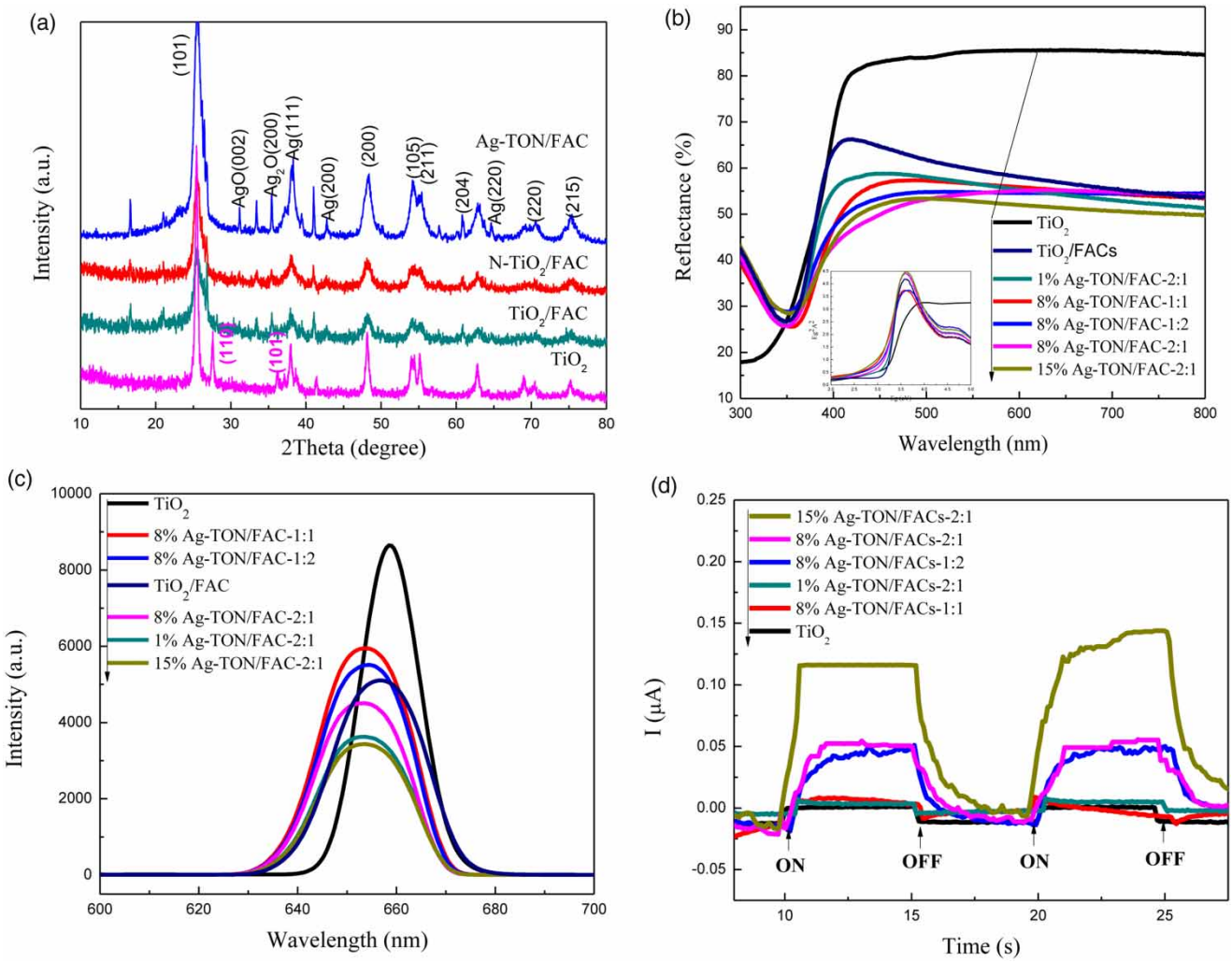

Figure 1 | Characterizations of samples (a) XRD; (b) UV–vis reflectance spectra and the bandgap diagram for the corresponding reflectance spectra; (c) FL spectra; (d) transient photocurrent response.

light below 388 nm, while the absorption peaks of Ag-TON/FAC extend to the visible light region and the absorption of the modified photocatalysts is red-shifted. Through modification with Ag and N, the band gaps are 2.87 eV (8% Ag-TON/FAC-2:1), 2.96 eV (8% Ag-TON/FAC-1:1), 3.07 eV (8% Ag-TON/FAC-1:2), 3.13 eV (1% Ag-TON/FAC-2:1) and 2.86 eV (15% Ag-TON/FAC-2:1) respectively. Their absorption band margins are 432 nm, 419 nm, 404 nm, 396 nm and 434 nm. Among these, the band gap of 15% Ag-TON/FAC-2:1 is the smallest, and has the most desired visible light absorption. The UV–vis reflectance spectra implies that the sample of Ag-TON/FAC can be easily excited under visible light and has better photocatalytic activity than TiO_2 and TiO_2/FAC because of the evident change of band gap. The obvious increase in visible light absorption capacity of the Ag-TON/FAC samples is due to the introduction of new energy levels by the incorporation of Ag and N in the band gap, resulting in additional energy states. These results indicate that the red-shift of absorption edge and narrowed band gap were achieved for TiO_2 with modification of Ag and N doping, which is beneficial to the visible-light-driven photocatalytic performance (Sun *et al.* 2017).

Figure 1(c) shows the photoluminescence emission spectra of all as-synthesized samples. FL emission spectra are used to investigate the capture, accumulation or transfer of electrons and holes in photocatalysts. All as-prepared composites show an emission peak at 655 nm, corresponding with its band gap energy of about 2.9 eV. In addition, the sample of pure TiO_2 has higher fluorescence emission intensity than composites, which means that the electron-hole pairs of TiO_2 have the fastest rate of photo-induced electrons recombining with holes (Gao *et al.* 2013). Compared with TiO_2, the peak intensity of Ag-TON/FAC reduces to a certain extent. The reason may be that the impurity energy level introduced to the top of the TiO_2 valence band and the separation of photogenerated electrons and holes can be effectively promoted. From Figure 1(c), the optimization ration of Ag-TON and FAC is 2:1, and the doping amount of Ag is 15 wt.%. The photoluminescence spectroscopy of 15% Ag-TON/FAC-2:1 has lower fluorescence emission intensity than other samples, which indicates that the separation efficiency of photogenerated carriers is further improved by the synergetic effect of Ag and N (Gao *et al.* 2018). It can be inferred that changing the doping amount of Ag reduces the photo-induced electron and hole recombination efficiency of the photocatalyst, which may be the main reason for the improving photocatalytic activity.

Figure 1(d) shows the transient photocurrent response of the as-synthesized samples. The transient photocurrent responses of the samples are evaluated for the separation of photogenerated electron–hole pairs and prolonged lifetime of carriers under visible light irradiation (Venkatkarthick *et al.* 2017). All the as-synthesized samples exhibit prompt photocurrent responses on each illumination and the photocurrent declines in dark. From Figure 1(d), it can be seen that the sample of 15% Ag-TON/FAC-2:1 shows a strong sensitivity to visible light, indicating that its photoelectric conversion activity is much stronger than that of the others. The enhanced photocurrent response demonstrates efficient charge separation and the photocatalytic activity will also increase accordingly, which is in accordance with the above-mentioned PL observation.

Figure 2 shows the SEM images of the as-synthesized samples. As shown in Figure 2(a), FAC has a spherical structure with a smooth surface and the particle size is

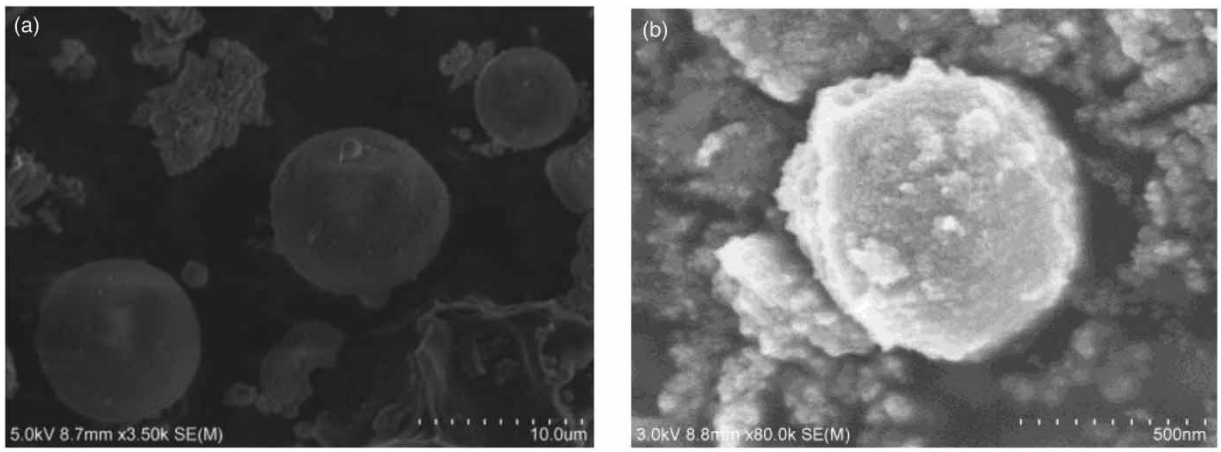

Figure 2 | The SEM of (a) FAC and (b) AgTON/FAC.

about 3–5 μm. In addition, the SEM image of Ag-TON/FAC (Figure 2(b)) shows that Ag-TON nanoparticles are successfully loaded on the surface of FAC, resulting in the roughness of FAC being significantly increased. The FAC maintain a good shape during solvothermal reaction even with the nanoparticles of Ag-TON coated on its surface uniformly dispersed. The particle size of the composite is about 500 nm. The dispersing and support of nano Ag-TON on FAC is beneficial to visible light degradation of waste, which will increase the absorption surface and reduce the aggregation of TiO_2 nanoparticles (Liu *et al.* 2016). This also facilitates the light absorption and at the same time it is beneficial in separating composites from the reaction system.

Figure 3 shows the photocatalytic degradation performance of MO and ciprofloxacin waste water. As shown in Figure 3(a), the photocatalytic activity of the sample in the dark is negligible. It is concluded that the sample of TiO_2/FAC has almost no ability to treat wastewater, while the removal efficiency of MO using 15% Ag-TON/FAC-2:1 reaches 87% within 180 min under visible light irradiation. From Figure 3(b), the photocatalytic degradation efficiency of ciprofloxacin is 48% (8% Ag-TON/FAC-1:2), 52% (8% Ag-TON/FAC-1:1), 65% (8% Ag-TON/FAC-2:1), 71% (1% Ag-TON/FAC-2:1) and 76% (15% Ag-TON/FAC-2:1), respectively. The ideal ratio of TiO_2 and FAC should be 2:1. The sample of 15% Ag-TON/FAC-2:1 has the highest reactive activity. This result corresponds to the transient

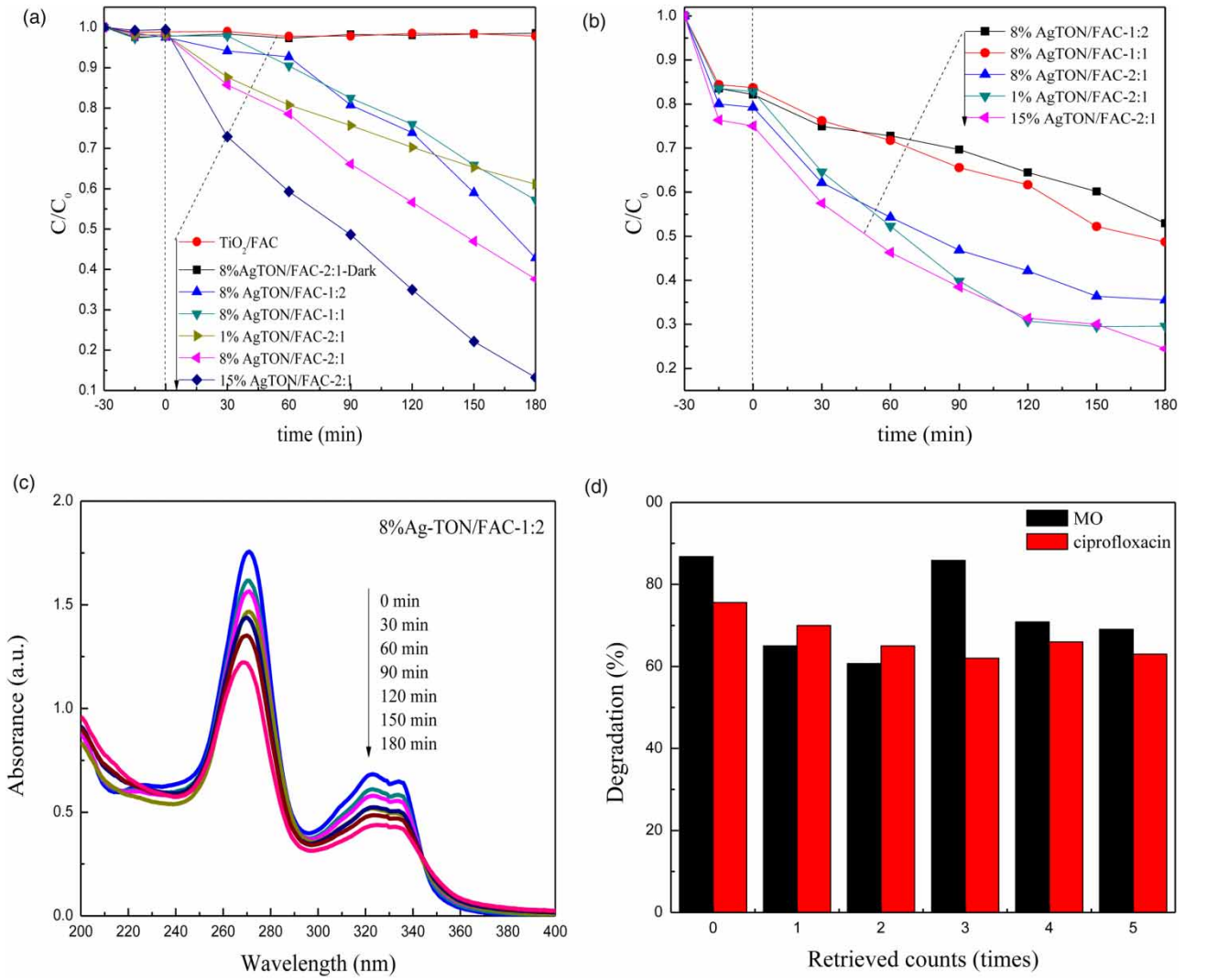

Figure 3 | Photocatalytic degradation activity of MO (a), ciprofloxacin (b) under irradiation of visible light, UV–vis spectra for degradation of ciprofloxacin (c) and recycle experiments of 15% Ag-TON/FAC-2:1 (d).

photocurrent response. It can be clearly seen from the absorption spectra of ciprofloxacin (Figure 3(c)) that the content of ciprofloxacin reduces with degradation time. Furthermore, the absorption spectra appears slightly blue-shifted (about 3 nm), indicating that the structure of ciprofloxacin is broken under visible light irradiation with the sample of Ag-TON/FAC. Different intermediates may form during the degradation process (Kansal *et al.* 2014). Figure 3(d) shows the recycle experiments for 15% Ag-TON/FAC-2:1 degradation of MO and ciprofloxacin. After each reaction, the composite is separated, washed three times with deionized water and then dried at 120 °C. As shown in Figure 3(d), the degradation efficiency maintains at more than 60% after being reused 5 times for MO and ciprofloxacin. The decrease of degradation may be attributed to the accumulation of MO or organic intermediates on the surface of photocatalysts and occupation of the active sites (Fan *et al.* 2018). It is clear that the degradation performance increased on the third time because the composite is heated at 450 °C for 2 h before it is reused. The increase of degradation may be attributed to high temperature removing the MO or organic intermediates accumulated on the surface of the composites. As shown in Figure 3(d), the degradation efficiency of ciprofloxacin wastewater is 76%, 70%, 65%, 62%, 66% and 63% for each time, respectively.

Doping of N might enhance the separation and transfer efficiency of the photogenerated carriers. The doped Ag is applied to act as an electron scavenger to inhibit the recombination of electron–hole pairs, and more holes are available for the oxidation reactions (Zhang *et al.* 2016). Changing the doping amount of silver can improve the photocatalytic effect. The enhanced photocatalytic property for the Ag-TON/FAC in the visible region is attributed to the localized surface plasmon resonance effect and a synergistic effect between Ag nanoparticles and N-TiO_2. In these experiments, FAC as a carrier provides good load conditions for nano TiO_2 and reduces the possibility of aggregation of nanoparticles.

CONCLUSION

Ag-TON/FAC nanoparticles are successfully prepared by a solvothermal and in-situ hydrolysis method. The optimal ratio of TiO_2 to FAC is 2:1 and the optimal doping ratio of Ag is 15 wt.%. The sample of 15% Ag-TON/FAC-2:1 presents an excellent visible light absorption covering the whole visible light range, and the degradation efficiencies under visible light irradiation after 180 min of MO and ciprofloxacin are 87% and 76%, respectively. This indicates that Ag-TON/FAC photocatalysts are suitable for treating organic wastewater and have potential application in dealing with environmental pollution.

ACKNOWLEDGEMENT

This work was partly supported by the National Natural Science Foundation of China (Grant no. 21605111), the National Science Foundation of Shanxi (Grant no. 2016011079), and also partly supported by the JSPS KAKENHI Grant Number JP16H06439 (Grant-in-Aid for Scientific Research on Innovative Areas), the Dynamic Alliance for Open Innovation Bridging Human, Environment and Materials, the Cooperative Research Program of 'Network Joint Research Center for Materials and Devices', TAGEN project.

REFERENCES

Achamo, T. & Yadav, O. P. 2016 Removal of 4-Nitrophenol from water using Ag-N-P-tridoped TiO_2 by photocatalytic oxidation technique. *Anal. Chem. Insights* **11** (11), 29–34.

Chen, F., Yang, Q., Li, X. Y., Zeng, G. M., Wang, D. B., Niu, C. G., Zhao, J. W., An, H. X., Xie, T. & Deng, Y. C. 2017 Hierarchical assembly of graphene-bridged Ag_3PO_4/Ag/$BiVO_4$ (040) Z-scheme photocatalyst: an efficient, sustainable and heterogeneous catalyst with enhanced visible-light photoactivity towards tetracycline degradation under visible light irradiation. *Appl. Catal. B-Environ.* **200**, 330–342.

Fan, H. G., Chen, D. D., Ai, X. F., Han, S., Wei, M. B., Yang, L. L., Liu, H. L. & Yang, J. H. 2018 Mesoporous TiO_2 coated $ZnFe_2O_4$ nanocomposite loading on activated fly ash cenosphere for visible light photocatalysis. *RSC Adv.* **8** (3), 1398–1406.

Fang, S. P., Zhou, Z. W., Xue, J. J., He, G. Y. & Chen, H. Q. 2018 Improved ciprofloxacin removal by a Fe(VI)-Fe_3O_4/graphene system under visible light irradiation. *Water Sci. Technol.* **2017** (2), 527–533.

Gao, Y. P., Fang, P. F., Chen, F. T., Liu, Y., Liu, Z., Wang, D. H. & Dai, Y. Q. 2013 Enhancement of stability of N-doped TiO_2 photocatalysts with Ag loading. *Appl. Surf. Sci.* **265** (2), 796–801.

Gao, D. W., Lu, Z. Q., Wang, C. X., Li, W. W. & Dong, P. Y. 2018 Enhanced photocatalytic properties of Ag-loaded N-doped TiO_2 nanotube arrays. *Autex Res. J.* **18** (1), 67–72.

Huo, P. W., Lu, Z. Y., Wang, H. Q., Pan, J. M., Li, H. M., Wu, H. Y., Huang, W. H. & Yan, Y. S. 2011 Enhanced photodegradation of antibiotics solution under visible light with Fe^{2+}/Fe^{3+}, immobilized on TiO_2/fly-ash cenospheres by

using ions imprinting technology. *Chem. Eng. J.* **172** (2), 615–622.

Ibrahim, M. M. & Asal, S. 2017 Physicochemical and photocatalytic studies of Ln^{3+}-ZnO for water disinfection and wastewater treatment applications. *J. Mol. Struct.* **1149**, 404–413.

Kanakaraju, D. & Wong, S. P. 2018 Photocatalytic efficiency of TiO_2-biomass loaded mixture for wastewater treatment. *J. Chem-NY.* **2018**, 1–14.

Kansal, S. K., Kundu, P., Sood, S., Lamba, R., Umar, A. & Mehta, S. M. 2014 Photocatalytic degradation of the antibiotic levofloxacin using highly crystalline TiO_2 nanoparticles. *New J. Chem.* **38** (7), 3220–3226.

Liu, S. M., Zhu, J. L., Yang, Q., Xu, P. P., Ge, J. H. & Guo, X. T. 2016 Synthesis and characterization of cube-like Ag@AgCl-doped TiO_2/fly ash cenospheres with enhanced visible-light photocatalytic activity. *Opt. Mater.* **53** (50), 73–79.

Ma, S., Hou, J. J., Yang, H. & Xu, Z. L. 2017 Preparation of renewable porous TiO_2/PVA composite sphere as photocatalyst for methyl orange degradation. *J. Porous Mat.* **25** (2018), 1071–1080.

Marques, N. J. O., Bellato, C. R., Souza, C. H. F., Silva, R. C. & Rocha, P. A. 2017 Synthesis, characterization and enhanced photocatalytic activity of iron oxide/carbon nanotube/Ag-doped TiO_2 nanocomposites. *J. Brazil. Chem. Soc.* **28** (12), 2301–2312.

Padmanaban, A., Dhanasekaran, T., Kumar, S. P., Gnanamoorthy, G., Munusamy, S., Stephen, A. & Narayanan, V. 2017 Visible light photocatalytic property of Ag/TiO_2 composite. *Mech. Mater. Sci. Eng. J.* **9** (1), 80–84.

Papoulis, D., Kordouli, E., Lampropoulou, P., Rapsomanikis, A., Kordulis, C., Panagiotaras, D., Theophylaktou, K., Stathatos, E. & Komarneni, S. 2014 Characterization and photocatalytic activities of fly ash-TiO_2 nanocomposites for the mineralization of azo dyes in water. *J. Surf. Inter. Mater.* **2** (4), 261–266.

Sieland, F., Schneider, J. & Bahnemann, D. W. 2018 Photocatalytic activity and charge carrier dynamics of TiO_2 powders with a binary particle size distribution. *PCCP* **20** (12), 8119–8132.

Sun, S. F., Sun, M. X., Kong, Y. Y., Liu, F. C., Yu, Z. S., Anandan, S. & Chang, C. 2017 One-step thermal synthesis of Ag-modified g-C_3N_4/N-doped TiO_2, hybrids with enhanced visible-light photocatalytic activity. *J. Mater. Sci.* **52** (2), 1183–1193.

Tang, Q., Meng, X. F., Wang, Z. Y., Zhou, J. W. & Tang, H. 2018 One-step electrospinning synthesis of TiO_2/g-C_3N_4 nanofibers with enhanced photocatalytic properties. *Appl. Surf. Sci.* **430**, 253–262.

Venkatkarthick, R., Davidson, D. J., Vasudevan, S., Sozhan, G. & Ravichandran, S. 2017 An investigation of interfacial and photoelectrochemical performance of thermally prepared C, N-codoped TiO_2 photoanodes for water splitting. *Chemistry Select* **2** (1), 288–294.

Wang, B., Li, Q., Wang, W., Li, Y. & Zhai, J. P. 2011 Preparation and characterization of Fe^{3+} doped TiO_2 on fly ash cenospheres for photocatalytic application. *Appl. Surf. Sci.* **257** (8), 3473–3479.

Wang, C. L., Hu, L. M., Chai, B. & Yan, J. T. 2018a Enhanced photocatalytic activity of electrospun nanofibrous TiO_2/g-C_3N_4 heterojunction photocatalyst under simulated solar light. *Appl. Surf. Sci.* **430**, 243–252.

Wang, D. B., Jia, F. Y., Wang, H., Chen, F., Fang, Y., Dong, W. B., Zeng, G. M., Li, X. M., Yang, Q. & Yuan, X. Z. 2018b Simultaneously efficient adsorption and photocatalytic degradation of tetracycline by Fe-based MOFs. *J. Colloid Interf. Sci.* **519**, 273–284.

Wu, Y. M., Xing, M. T., Tian, B. Z., Zhang, J. L. & Chen, F. 2010 Preparation of nitrogen and fluorine co-doped mesoporous TiO_2 microsphere and photodegradation of acid orange 7 under visible light. *Chem. Eng. J.* **162** (2), 710–717.

Yu, H. B., Huang, B. B., Wang, H., Yuan, X. Z., Jiang, L. B., Wu, Z. B., Zhang, J. & Zeng, G. M. 2018 Facile construction of novel direct solid-state Z-scheme AgI/BiOBr photocatalysts for highly effective removal of ciprofloxacin under visible light exposure: mineralization efficiency and mechanisms. *J. Colloid Interf. Sci.* **522**, 82–94.

Zhang, J., Wang, X. J., Xia, P., Wang, X., Huang, J. Y., Chen, J., Louangsouphom, B. & Zhao, J. F. 2016 Enhanced sunlight photocatalytic activity and recycled Ag–N co-doped TiO_2, supported by expanded graphite C/C composites for degradation of organic pollutants. *Res Chem. Intermediat* **42** (6), 1–17.

Zhang, J., Liu, F., Gao, J. M., Chen, Y. & Hao, X. M. 2017 Ordered mesoporous TiO_2/activated carbon for adsorption and photocatalysis of acid red 18 solution. *Bioresources* **12** (4), 9086–9102.

Zhao, Z. H., Lei, Y. Y., Liu, W. H., Fan, J. M., Xue, D. F., Xue, Y. Q. & Yin, S. 2017 Fly ash cenospheres as multifunctional supports of g-C_3N_4/N-TiO_2 with enhanced visible-light photocatalytic activity and adsorption. *Adv. Powder Technol.* **28** (12), 3233–3240.

Zhou, J. S., Li, F. Z., Du, C., Liu, J. M., Wang, Y. Z., Li, W., He, G. N. & He, Q. Y. 2016 Photodegradation performance and recyclability of a porous nitrogen and carbon co-doped TiO_2/activated carbon composite prepared by an extremely fast one-step microwave method. *RSC Adv.* **6** (87), 84457–84463.

First received 30 July 2018; accepted in revised form 6 December 2018. Available online 17 December 2018